Radiology

Management of Nodules Attached to the Costal Pleura at Low-Dose CT Screening for Lung Cancer

Yeqing Zhu, MD, PhD • Rowena Yip, MPH • Nan You, MS • Claudia I. Henschke, MD, PhD • David F. Yankelevitz, MD

From the Department of Radiology, Icahn School of Medicine at Mount Sinai, One Gustave L. Levy Place, Box 1234, New York, NY 10029-6574. Received May 29, 2020; revision requested June 19; final revision received July 24; accepted August 14. **Address correspondence to** D.F.Y. (e-mail: *david.yankelevitz@mountsinai.org*).

Supported in part by the Simons Foundation.

Conflicts of interest are listed at the end of this article.

See also the editorial by Godoy in this issue.

Radiology 2020; 297:710–718 • https://doi.org10.1148/radiol.2020202388 • Content codes: CH CT

Background: Pulmonary nodule features have been used to differentiate benign from malignant nodules.

Purpose: To determine the frequency of solid noncalcified nodules attached to the costal pleura (CP-NCNs) at baseline low-dose CT and to identify key features of benignity.

Materials and Methods: A retrospective review was performed of baseline low-dose CT scans obtained in 8730 participants in the Mount Sinai Early Lung and Cardiac Action Program screening cohort between 1992 and 2019. Participants with one or more solid CP-NCNs between 3.0 mm and 30.0 mm in average diameter were included. For each CP-NCN, the size, location, shape (lentiform, oval, or semicircular [LOS]; triangular; polygonal; round; or irregular), margin (smooth or nonsmooth), and attachment to the costal pleura (broad or narrow) were documented. The manifestation of emphysema and fibrosis within a 10-mm radius of the CP-NCN was determined. Multivariable logistic regression analysis, with synthetic minority oversampling techniques, was used.

Results: The 569 eligible participants (average age, 62 years ± 9 [standard deviation]; 343 women) had 943 solid CP-NCNs, of which 934 (99.0%) were benign and nine (1.0%) were malignant. Multivariable analysis showed that five shapes could be consolidated into three (LOS and/or triangular, round and/or polygonal, and irregular shape); pleural attachment was not a significant independent predictor (odds ratio, 1.24; $P = .70$); and interaction terms of size with shape (odds ratio, 0.73; $P = .005$) and margin were significant (odds ratio, 0.80; $P = .001$). All 603 CP-NCNs less than 10.0 mm with LOS or triangular shapes and smooth margins were benign.

Conclusion: All baseline noncalcified solid nodules attached to the costal pleura less than 10.0 mm in average diameter with lentiform, oval, semicircular, or triangular shapes and smooth margins were benign; thus, for these nodules, an annual repeat scan in 1 year, rather than a more immediate work-up, is recommended.

Online supplemental material is available for this article.

Low-dose CT screening for the early detection of lung cancer in at-risk individuals has been approved for reimbursement in the United States and implemented throughout the country. To maximize the benefit of low-dose CT screening, efficient management regimens are needed that minimize unnecessary work-up between screening rounds, while still identifying small early-stage lung cancers. Extensive efforts have been made to differentiate benign from malignant pulmonary nodules. This differentiation was first based on features on chest radiographs obtained in both clinical care (1,2) and screening (3) settings, and then starting in the 1980s, it was based on chest CT findings (4–6). These efforts intensified with the approval of low-dose CT screening. Initial criteria were based on size, as used in the Early Lung Action Program Project protocol (7), and then nodule consistency was added (8); these criteria were updated as additional evidence emerged from screening studies (9,10).

Data from the Nagano Prefecture screening study (11) indicated that pulmonary nodules with a polygonal shape and smooth margin suggested benignity (12,13). Later, perifissural nodules (PFNs), which represent about 20% of pulmonary nodules, were identified as benign (14–18). PFNs have been defined as solid homogeneous nodules attached or in close proximity to a fissure, having a lentiform, oval, or semicircular (LOS) or a triangular shape and smooth margins. Several guidelines have noted that PFNs less than 10 mm in diameter should be recommended for 1-year follow-up, rather than for more immediate work-up (19–22). Although it might be assumed that nodules attached to the costal pleura with similar features would have a similar rate of benignity, the American College of Radiology Lung CT Screening Reporting and Data System Committee stated that they needed to collect further evidence before making their recommendations for costal pleural–based nodules (22).

We aimed to determine the frequency of solid noncalcified nodules attached to the costal pleura (CP-NCNs) at low-dose CT between 3.0 mm and 30.0 mm in average diameter in the Mount Sinai Early Lung and Cardiac Action Program and to identify features to help distinguish benign from malignant CP-NCNs and develop appropriate recommendations for follow-up.

Materials and Methods

The participants in this retrospective study were identified among all Mount Sinai Early Lung and Cardiac

Abbreviations

CI = confidence interval; CP-NCN = noncalcified nodule attached to the costal pleura; LOS = lentiform, oval, or semicircular; PFN = perifissural nodule

Summary

At baseline low-dose CT screening, all noncalcified nodules attached to the costal pleural less than 10.0 mm in diameter with lentiform, oval, semicircular, or triangular shapes with smooth margins were benign.

Key Results

- Five types of lung nodule shapes can be consolidated into three types: *(a)* lentiform, oval, or semicircular (LOS) and triangular; *(b)* round and polygonal; and *(c)* irregular.
- Of the 897 noncalcified nodules attached to the costal pleura that were less than 10.0 mm in diameter at baseline low-dose CT, all 603 (67.2%) with LOS or triangular shapes and smooth margins were benign.

Action Program participants (n = 8730) who signed consent forms between 1992 and 2019. The study was approved by the institutional review board and compliant with the Health Insurance Portability and Accountability Act. Participants did not undergo CT in the past 3 years and were *(a)* asymptomatic, *(b)* 40 years of age or older, *(c)* current and former smokers as well as never smokers who had occupational or secondhand tobacco smoke exposure, *(d)* never diagnosed with lung cancer, and *(e)* fit to undergo thoracic surgery. If cancers other than lung cancer had been previously diagnosed, then participants were eligible if they had been curatively treated 5 or more years before enrollment. Other abnormalities (aortic valve calcification, hepatic steatosis, and adrenal enlargement or mass) in the Mount Sinai Early Lung and Cardiac Action Program database have been reported elsewhere (23–25). Documented at baseline enrollment were sex, age, smoking history, and self-reported comorbidities. Baseline low-dose CT interpretation had been performed by an experienced board-certified attending chest radiologist who documented nodule location, size, and distance to the pleura in the Mount Sinai Early Lung and Cardiac Action Program database. Work-up was performed according to the International Early Lung Cancer Action Program protocol (26), and interventions and diagnoses of lung cancer were documented. A data scientist (R.Y., with 18 years of experience) searched the Mount Sinai Early Lung and Cardiac Action Program database and identified 905 participants who had one or more noncalcified nodules reported to be 0 mm from the pleura among the 8730 participants. After review, 168 participants with CP-NCNs less than 3.0 mm in diameter, six with CP-NCNs greater than 30.0 mm in diameter, and 162 with nodules that did not meet the CP-NCN criteria were excluded. This left 569 included participants with 943 solid CP-NCNs between 3.0 mm and 30.0 mm in average diameter (Fig 1).

CT Imaging

Baseline low-dose CT scans were obtained at 140 kVp or less and at 80 mAs or less by using multidetector row CT scanners (HiSpeed Advantage, LightSpeed; GE Healthcare, Waukesha, Wis and Somatom Definition Flash; Siemens Healthineers, Erlangen, Germany) in a single breath hold, from the lung apices to the upper abdomen, at maximum inspiration without intravenous contrast material. CT images were reconstructed at axial slice thickness of 1.25 mm or less.

Image Assessment of Baseline Low-Dose CT Images

The baseline low-dose CT scans were rereviewed by one radiologist (Y.Z., with 8 years of chest radiology and 2 years of lung cancer screening experience) who was blinded to clinical information and final diagnoses, using window settings for lung (width, 1500 HU; level, −650 HU) and mediastinum (width, 400 HU; level, 35 HU) on picture archiving and communication system workstations (GE Healthcare). Distance from the pleura was defined by the shortest line from the nodule perpendicular to the pleura (27) (Fig 2, *A* and *B*). Nodules with fine linear septal extensions to the pleura (Fig 2, *B*) were excluded if the nodule itself did not touch the costal pleura.

For each CP-NCN, one radiologist (Y.Z.) determined size, shape, margin, type of pleural attachment, and presence of parenchymal emphysema or fibrosis within a 10-mm radius of the CP-NCN.

Size was the average of the maximum length and maximum width, which was perpendicular to the length on the axial image showing the maximum area of the CP-NCN (26).

Shape was classified into five types, as follows: *(a)* round (width divided by the length was greater than 0.66) (Fig 3, *A* [7]); *(b)* lentiform (lentil shaped) (Fig 3, *B* [16]), oval (if the width divided by length was less than 0.66 [7]), or semicircular (convex toward the lung and had a broad pleural attachment; these three shapes have been abbreviated as LOS herein) (Fig 3, *C* [15]); *(c)* triangular (three cornered) (Fig 3, *D* [16]); *(d)* polygonal (nodule borders with the lung were straight or concave [eg, trapezoidal, rectangular, or pentagonal]) (Fig 3, *E* [12]); or *(e)* irregular (CP-NCN did not meet any of the criteria for the other shapes) (Fig 3, *F*).

The margin was defined as either smooth (sharp and distinct) or nonsmooth (irregular or the contour had abrupt bulging [28], or multiple thin linear strands extending from the CP-NCNs [29]).

The type of pleural attachment was determined using the length of the CP-NCN along the pleura and its length along the nodule (Fig 4) (14,30). The type of pleural attachment was classified as broad if the length along the pleura divided by the length along the nodule was at least 0.5. Attachment was classified as narrow if the length along the pleura divided by the length along the nodule was less than 0.5.

The presence of parenchymal emphysema or fibrosis within a 10-mm radius of the CP-NCN was determined as follows: Emphysema was determined to be present if the lung parenchyma within a 10-mm radius of the CP-NCN had low attenuation regions. If reticular changes were present, then fibrosis was manifested.

Statistical Analysis

The analyses were performed by two data scientists (R.Y., with 18 years of experience and N.Y., with 4 years of experience)

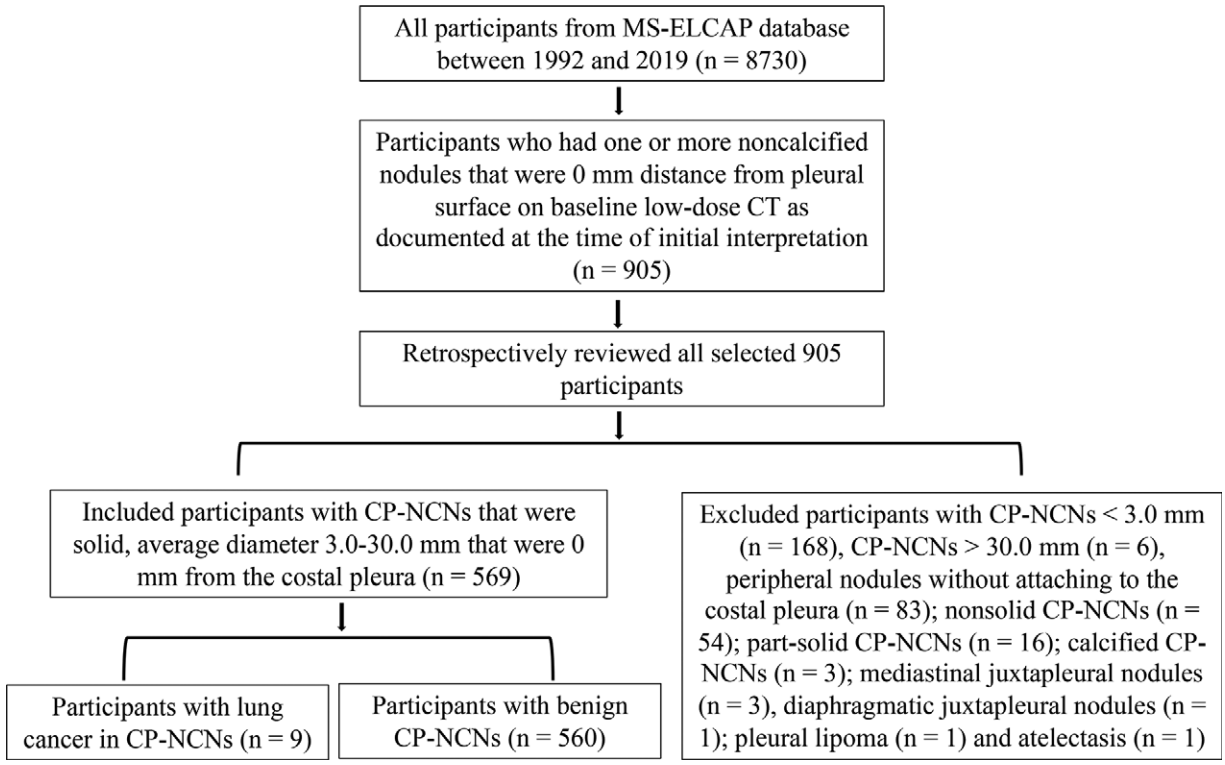

Figure 1: Flowchart of identification process of 569 screening participants with one or more noncalcified nodules attached to costal pleura (CP-NCNs) at baseline low-dose CT. MS-ELCAP = Mount Sinai Early Lung and Cardiac Action Program.

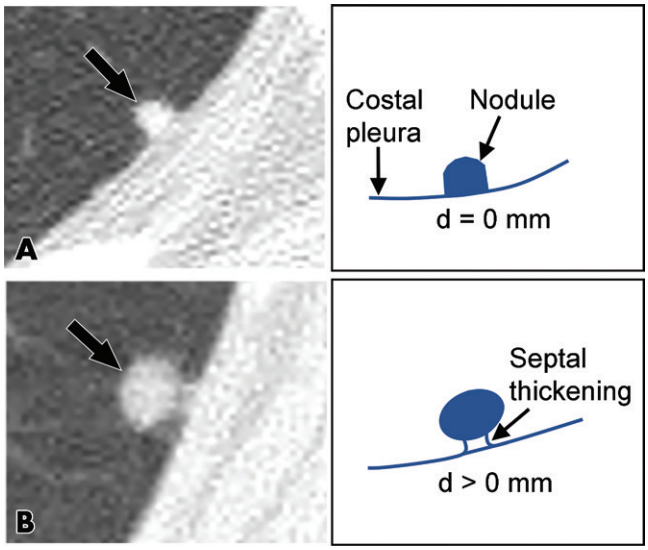

Figure 2: Images show examples of a solid noncalcified nodule attached to costal pleura (CP-NCN) and a non–CP-NCN. *A*, Low-dose CT image of solid CP-NCN (arrow) with 0-mm distance from costal pleura. Diagram is also shown. *B*, Low-dose CT image indicates non–CP-NCN because distance from nodule (arrow) to adjacent costal pleura is more than 0 mm, even though it has fine linear septal extensions to pleura. Diagram is also shown. Note that *d* denotes distance from pleura as defined as length of shortest perpendicular line drawn from nodule to costal pleura.

to identify features of benign CP-NCNs. Categorical variables are summarized as frequencies and percentages; continuous variables are summarized by means ± standard deviations for normally distributed data or by the median and interquartile range for nonparametric data. Continuous variables were assessed for normal distribution with the Shapiro-Wilk test. Differences in features of benign and malignant CP-NCNs were compared by using the χ^2 test or Fisher exact test for categorical variables. The Student *t* test or Wilcoxon rank sum test was used for parametric and nonparametric continuous variables. All participants were followed up annually according to the study protocol. Cancer diagnosis and/or date and cause of death was obtained from the participant's physician, family members, or both. For verification and loss to follow-up, the National Death Index was searched. Follow-up time was calculated from baseline CT to date of lung cancer diagnosis, date of death, or December 31, 2019, whichever came first.

To address the imbalance of the data due to low prevalence of lung cancers, the synthetic minority oversampling technique was applied, and multivariable logistic regression analysis was used. Odds ratios and corresponding 95% confidence intervals (CIs) were determined. To assess the interactions between shape, margin, and benignity of CP-NCN by size, interaction terms of shape × size and margin × size were included in the model. The Firth penalized maximum likelihood estimation method was used. To prevent inflation of the type I error rate in the multiple comparison test, adjusted *P* values for comparison of all possible pairwise differences of shapes were computed by using the Tukey-Kramer method. $P < .05$ was considered to be a statistically significant difference. Predicted probabilities of benignity were calculated by using the final multivariable logistic regression model. All analyses were performed by using SAS software (version 9.4; SAS Institute, Cary, NC) and R software (version 3.6.3; R Foundation for Statistical Computing, Vienna, Austria).

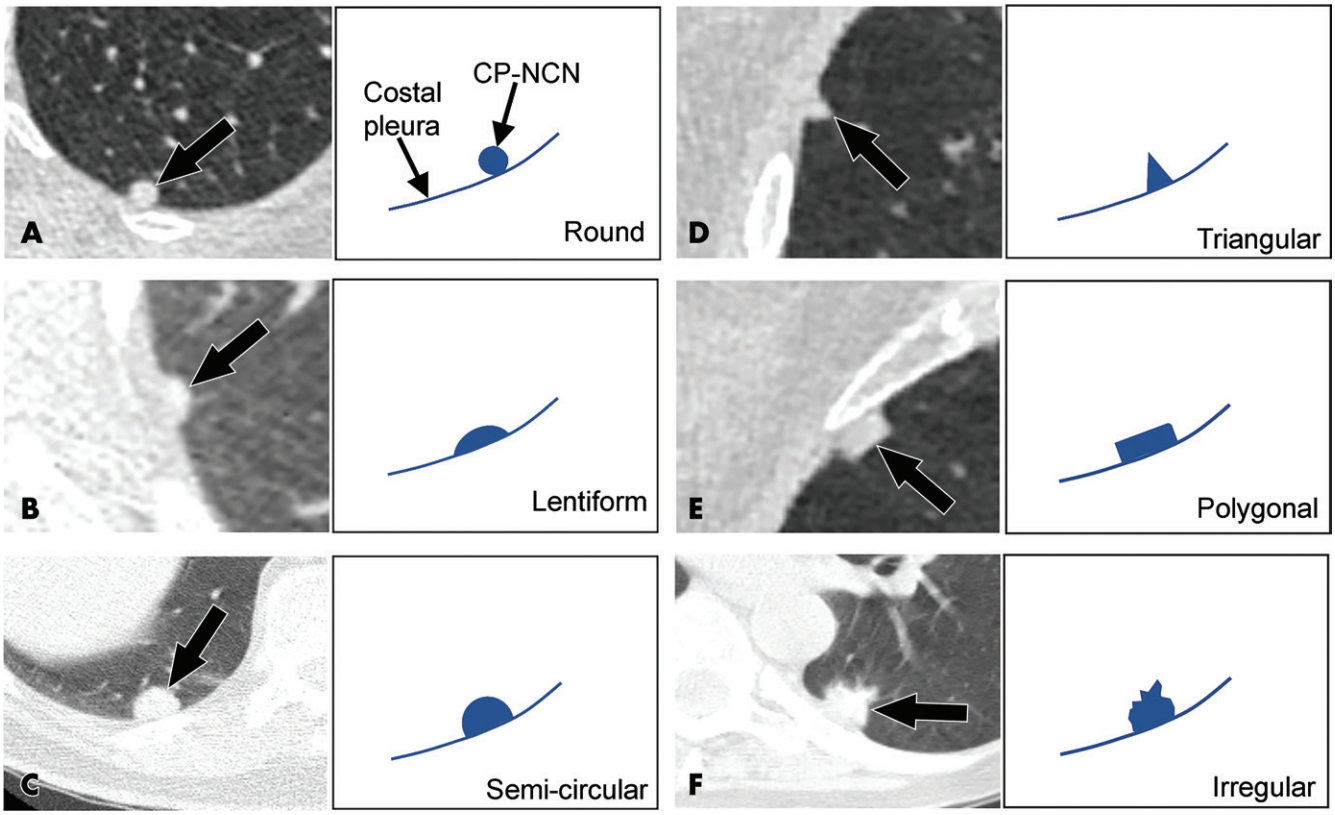

Figure 3: CT scans and corresponding diagrams demonstrate shapes of noncalcified nodules attached to costal pleural (CP-NCNs) (arrow). Nodules are, *A*, round, as width divided by length was greater than 0.66; *B*, lentiform, as having a lentil shape; *C*, semicircular, as it was convex toward lung and had broad pleural attachment; *D*, triangular, as it was three cornered; *E*, polygonal, as its borders with lung were straight and concave; and, *F*, irregular, as none of the shapes given in *A–E* applied.

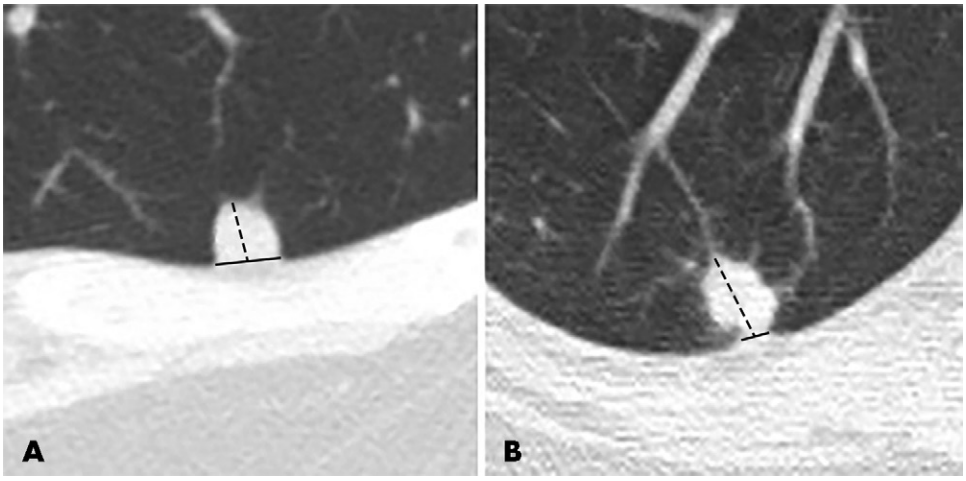

Figure 4: Images show determination of type of pleural attachment. Maximum length of nodule and pleura contact (solid line) and maximum length of nodule (dashed line) were measured on axial low-dose CT images. Attachment was, *A*, broad if length of nodule and pleura contact divided by length of nodule was greater than 0.5, and, *B*, narrow if length of nodule and pleura contact divided by length of nodule was less than 0.5.

Results

Overview of Participant Characteristics

Among 8730 screening participants, 569 (7%) had at least one solid CP-NCN of 3.0–30.0-mm in average diameter at baseline low-dose CT. The mean age was 62.1 years ± 8.8, and 343 (60%) were women (Table 1). The 569 participants had a total of 943 solid CP-NCNs; 345 (61%) had one CP-NCN, 136 (24%) had two CP-NCNs, and 88 (16%) had three or more CP-NCNs. Nine participants had stage I lung cancer diagnosed in a CP-NCN, and none had more than one malignant CP-NCN. Details of the shape, margin, diagnoses, and treatment are given in Table 2. Lung cancer was more frequent in former smokers than in current smokers (89% [eight of nine] vs 11% [one of nine]; P = .02); no lung cancer occurred in never smokers. Median pack-years of smoking was higher for participants with a malignant CP-NCN than for those with benign CP-NCNs (60.0 pack-years vs 29.5 pack-years; P = .001). Median follow-up time for all 569 participants was 7.8 years (interquartile range, 3.1–16.9 years). The median follow-up time was 1.6 years (interquartile range, 0.1–2.7 years) for the nine participants with a malignant CP-

Table 1: Characteristics of Participants with Largest CP-NCN at Baseline Low-Dose CT and Frequency of Lung Cancer Originated from CP-NCN per Participant

Parameter	Total	Participants with Benign CP-NCNs (*n* = 560)	Participants with Lung Cancer in CP-NCNs (*n* = 9)	*P* Value
Participant characteristics				
Sex				.99
Men	226 (40)	223 (40)	3 (33)	…
Women	343 (60)	337 (60)	6 (67)	…
Age (y)*	62.1 ± 8.8	62.1 ± 8.8	63.7 ± 5.9	.42
Smoking status				.02
Current smoker	227 (40)	226 (40)	1 (11)	…
Former smoker	231 (41)	223 (40)	8 (89)	…
Never smoker	111 (20)	111 (20)	0 (0.0)	…
Pack-years of smoking†	30.0 (7.5–45.0)	29.5 (6.9–45.0)	60.0 (47.0–86.0)	.001
Comorbid conditions				
COPD	92 (16)	91 (16)	1 (11)	.99
Diabetes	60 (11)	58 (10)	2 (22)	.24
Cardiac disease	29 (5)	29 (5)	0 (0.0)	>.99
Vascular disease	131 (23)	131 (23)	0 (0.0)	.13
Other diseases	187 (33)	185 (33.0)	2 (22)	.72
Cancers other than lung	83 (15)	80 (14)	3 (33)	.13
Lung cancer in non–CP-NCN	20 (4)	19 (3)	1 (11)	.28
CT findings				
No. of CP-NCNs				
Median†	1 (1–2)	1 (1–2)	1.0 (1–2)	.89
1	345 (61)	339 (61)	6 (67)	.63
2	136 (24)	135 (24)	1 (11)	…
≥3	88 (16)	86 (15)	2 (22)	…
Average diameter of largest CP-NCN (mm)				<.001
3.0–5.9	435 (76)	433 (77)	2 (22)	…
6.0–9.9	89 (16)	88 (16)	1 (11)	…
10.0–14.9	29 (5)	26 (5)	3 (33)	…
15.0–30.0	16 (3)	13 (2)	3 (33)	…

Note.—Except where indicated, data are numbers of participants, with percentages in parentheses. COPD = chronic obstructive pulmonary disease, CP-NCN = noncalcified nodules attached to the costal pleura.

* Numbers are means ± standard deviations.

† Numbers are medians, with interquartile ranges in parentheses.

NCN and 7.8 years (interquartile range, 3.2–17.1 years) for the 560 participants with benign CP-NCNs.

CP-NCN Characteristics

Among the 943 CP-NCNs, 934 (99.0%; 95% CI: 98.2%, 99.6%) were benign and nine (1.0%; 95% CI: 0.4%, 1.8%) were malignant (Table 3). Most benign CP-NCNs (*n* = 934) were between 3.0 mm and 5.9 mm (782 [83.7%]), while some were larger (112 [12%] were 6.0–9.9 mm, 27 [2.9%] were 10.0–14.9 mm, and 13 [1.4%] were 15.0–30.0 mm). Significant CP-NCNs features associated with benignity were size ($P < .001$), shape ($P < .001$), and margin ($P < .001$); lobe location ($P = .14$) and type of pleural attachment ($P = .24$) were not significant. Perinodular emphysema was less frequent in benign than in malignant CP-NCNs (13.4% vs 77.8%; $P < .001$), while fibrosis was only seen in benign CP-NCNs (2.7% vs 0%; $P = .99$).

The frequency of benign nodules decreased with increasing size, from 99.7% (782 of 784 nodules; 95% CI: 99.1%, 100%) for CP-NCNs measuring 3.0–5.9 mm to 99.1% (112 of 113 nodules; 95% CI: 95.2%, 100%) for CP-NCNs measuring 6.0–9.9 mm, 90% (27 of 30 nodules; 95% CI: 69%, 98%) for CP-NCNs measuring 10.0–14.9 mm, and 81% (13 of 16 nodules; 95% CI: 54%, 96%) for CP-NCNs measuring 15.0–30.0 mm. Table 3 also shows that the frequency of benign CP-NCNs by shape decreased from 100% (95% CI: 98.8%, 100%) for 317 of 317 triangular CP-NCNs to 99.7% (95% CI: 98.2%, 100%) for 311 of 312 LOS CP-NCNs, to 99.0% (95% CI: 96.5%, 99.9%) for 199 of 201 polygonal CP-NCNs, to 99% (95% CI: 93%, 100%) for 73 of 74 round CP-NCNs, and to 87% (95% CI: 73%, 96%) for 34 of 39 irregular CP-NCNs. Finally, of the 885 CP-NCNs with smooth margins, 882 (99.7%; 95% CI: 99.0%, 99.9%) of them were benign.

Table 2: Location, Size, and Features of Malignant CP-NCNs, Time to Diagnosis after Baseline Low-Dose CT, Cell Type, and Treatment

Participant No.	Lobe	Average Diameter (mm)	Shape	Margin	Pleural Attachment	Emphysema*	Fibrosis*	Time to Diagnosis (mo)	Cell Type	Pathology Stage (8th Ed)	Treatment
1	LUL	3.5	Polygonal	Smooth	Broad	Centrilobular	No	25	AC	T1aN0M0	Surgery
2	RLL	5.6	Round	Nonsmooth	Narrow	Centrilobular	No	20	SCC	T2N0M0	Surgery
3	RUL	7.0	Polygonal	Smooth	Broad	Centrilobular	No	32	AC	T1N0M0	Surgery
4	RUL	10.7	Irregular	Nonsmooth	Narrow	Centrilobular	No	0	AC	T1N0M0	Surgery
5	RLL	12.5	Semicircular	Smooth	Broad	No	No	49	AC	T1N0M0	Surgery
6	RLL	13.2	Irregular	Nonsmooth	Broad	No	No	39	AC	T1bN0M0	Surgery
7†	LUL	16.9	Irregular	Nonsmooth	Broad	Centrilobular and paraseptal	No	0	AC	T1N0M0	Radiation therapy‡
8	RLL	24.3	Irregular	Nonsmooth	Broad	Centrilobular and paraseptal	No	2	AC	T2bN0M0	Surgery
9	RUL	29.2	Irregular	Nonsmooth	Broad	Centrilobular and paraseptal	No	1	AC	T1N0M0	Surgery

Note.—AC = adenocarcinoma, CP-NCN = noncalcified nodule attached to the costal pleura, Ed = edition, LUL = left upper lobe, RLL = right lower lobe, RUL = right upper lobe, SCC = squamous cell carcinoma.

* Both emphysema and fibrosis were within 1 cm of the nodule.

† Participant had a second lung cancer in a non–CP-NCN, attached to the mediastinal pleural in the opposite lung.

‡ Participant underwent radiation therapy rather than surgery because of multiple lung cancers (adenocarcinoma in LUL CP-NCN and squamous cell carcinoma in RUL non–CP-NCN).

Multivariable logistic regression analysis with synthetic minority oversampling technique showed that LOS, triangular, and polygonal shapes were significantly different from irregular shape and that smooth margin was significantly different from nonsmooth margin ($P < .001$) in probability of benignity, but type of pleural attachment was not ($P = .70$) (Table 4).

Multivariable analysis showed that the interaction terms between size and margin ($P = .001$) and between size and shape ($P = .005$) were significant. Thus, odds ratios of shape and margin depended on the size of the CP-NCN and needed to be estimated for particular feature and size combinations (Table E1 [online]). When compared with an irregularly shaped CP-NCN, the odds ratio for benignity for those with LOS shape decreased with increasing nodule size, from 30.5 (95% CI: 9.9, 93.8) for a 6.0-mm CP-NCN, to 21.6 (95% CI: 9.2, 50.8) for a 10.0-mm CP-NCN, and to 14.0 (95% CI: 4.9, 40.0) for a 15.0-mm CP-NCN. Similarly, compared with CP-NCNs with a nonsmooth margin, the odds ratio for benignity of CP-NCNs with a smooth margin was 9.1 (95% CI: 4.4, 18.9) for 6.0-mm CP-NCNs, and it decreased to 3.8 (95% CI: 2.0, 7.1) for 10.0-mm CP-NCNs and to 1.3 (95% CI: 0.5, 3.5) for 15.0-mm CP-NCNs.

Table E2 (online) also gives the probability of benignity for different shape comparisons. All were significantly different except for LOS versus triangular ($P = .48$) and polygonal versus round ($P = .98$) shapes, suggesting that the five shapes could be consolidated into three: *(a)* LOS or triangular, *(b)* round and polygonal, and *(c)* irregular. Using these three consolidated shape categories, we determined the frequency of benignity among the 897 CP-NCNs less than 10.0 mm and found that all 603 (67.2%) CP-NCNs with LOS or triangular shapes and smooth margins were benign. Among 263 participants with CP-NCNs less than 10.0 mm in diameter with round or polygonal shapes, 260 participants (98.9%) had benign CP-NCNs. The three malignant CP-NCNs were one round CP-NCN with a nonsmooth margin and two polygonal CP-NCNs with smooth margins. These malignant CP-NCNs were diagnosed as stage I lung cancers 20, 25, and 32 months after the baseline low-dose CT scan.

Discussion

Our analysis showed that among 8730 participants enrolled in a screening program, 569 had 943 noncalcified nodules attached to the costal pleura (CP-NCNs) identified at baseline CT. Of the 943 CP-NCNs, 897 were less than 10.0 mm, and all 603 CP-NCNs with lentiform, oval, or semicircular or triangular shapes and smooth margins were benign. According to this evidence, we recommend follow-up with annual screening for these CP-NCNs rather than more immediate work-up.

Li and colleagues (13) reported on 137 solid nodules of 3–20 mm in size in the Nagano screening study. They found that oval or polygonal nodules with smooth margins were more frequently benign than nodules of other shapes, which is similar to our results. However, they did not distinguish between CP-NCNs and other nodules in the lungs. Later, the Dutch-Belgian Randomized Lung Cancer Screening Trial investigators (14) reported 658 participants who had 155 pleural-attached nodules, 4.6–9.8 mm in diameter, at baseline low-dose CT and at annual repeat low-dose CT 1 year later. None were found to be malignant, a result similar to ours.

Schreuder et al (31) evaluated the interreader variability of PFNs by using a cancer-enriched subset of the National Lung Screening Trial database. Among 1067 lung cancer nodules, 323 had been scanned with a slice thickness of less than 2 mm, and among the 323 cancer nodules, 70 had an average diameter of 5–10 mm. Fifteen of those 70 nodules were attached to the

Table 3: Features of All CP-NCNs at Baseline Low-Dose CT

CP-NCN Features	Total (n = 943)	Benign CP-NCNs (n = 934)	Lung Cancer in CP-NCNs (n = 9)	P Value
Nodule size (mm)				
Median*	4.2 (3.5–5.4)	4.2 (3.5–5.3)	12.5 (7.0–16.9)	<.001
3.0–5.9	784 (83.1)	782 (83.7)	2 (22)	<.001
6.0–9.9	113 (12.0)	112 (12.0)	1 (11)	…
10.0–14.9	30 (3.2)	27 (2.9)	3 (33)	…
15.0–30.0	16 (1.7)	13 (1.4)	3 (33)	…
Shape, in decreasing frequency				
Triangular	317 (33.6)	317 (33.9)	0 (0)	<.001
Lentiform, oval, or semicircular	312 (33.1)	311 (33.3)	1 (11)	…
Polygonal	201 (21.3)	199 (21.3)	2 (22)	…
Round	74 (7.8)	73 (7.8)	1 (11)	…
Irregular	39 (4.1)	34 (3.6)	5 (56)	…
Margin				
Smooth	885 (93.8)	882 (94.4)	3 (33)	<.001
Nonsmooth	58 (6.2)	52 (5.6)	6 (67)	…
Nodule-pleural attachment				
Broad	845 (89.6)	838 (89.7)	7 (78)	.24
Narrow	98 (10.4)	96 (10.3)	2 (22)	…
Adjacent parenchyma findings (<10 mm of the nodule)				
Perinodular emphysema	132 (14.0)	125 (13.4)	7 (78)	<.001
Perinodular fibrosis	25 (2.7)	25 (2.7)	0 (0)	.99
Nodule location				
RUL or RML	262 (27.8)	259 (27.7)	3 (33)	.14
RLL	293 (31.1)	289 (30.9)	4 (44)	…
LUL	112 (11.9)	110 (11.8)	2 (22)	…
LLL	276 (29.3)	276 (29.6)	0 (0)	…
Upper or middle	374 (39.7)	369 (39.5)	5 (56)	.33
Lower	569 (60.3)	565 (60.5)	4 (44)	…

Note.—Table shows that size, shape, margin, and presence of emphysema are important differences between benign and malignant nodules. Except where indicated, data are numbers of nodules, with percentages in parentheses. CP-NCN = noncalcified nodules attached to the costal pleura, LLL = left lower lobe, LUL = left upper lobe, RLL = right lower lobe, RML = right middle lobe, RUL = right upper lobe.

* Numbers in parentheses are interquartile ranges.

pleura (the particular pleural attachment was not reported). The six readers were asked to classify each of the 70 cancers as being *(a)* a typical PFN (lentiform, triangular, or polygonal shape; located on or within 10 mm of the visceral pleura or lung fissure, with extending linear densities), *(b)* an atypical PFN (lacked one of the three key criteria defining a typical PFN), or *(c)* a non-PFN. A PFN could neither have spiculations, an irregular shape, or an unsharp border, nor could it distort the pleura or fissure. None of the six readers found that the 15 pleural-attached cancer nodules met the criteria of being a typical PFN. Two of the six readers each found one case that met the criteria of an atypical PFN. Thus, none of the 15 pleural-attached cancers had a typical PFN appearance or met the criteria we established that all CP-NCNs less than 10.0 mm with LOS or triangular shapes and smooth margins were benign. Their results also agree with ours.

Our recommendations based on 943 CP-NCNs extend the current Lung CT Screening Reporting and Data System version 1.1 (22) recommendations, which classify solid fissure–attached nodules with smooth margins less than 10.0 mm with LOS or triangular shapes as category 2 nodules for which 1-year follow-up is recommended. Lung CT Screening Reporting and Data System version 1.1 based its recommendations on 794 typical PFNs and 125 atypical PFNs (16), of which the frequency of costal pleural nodules is unknown. Our recommendation is consistent with the current Fleischner recommendations for incidentally detected PFNs or juxtapleural nodules at CT in adult patients at least 35 years old (20,21), regardless of smoking history, similar to our screening eligibility criteria. The Fleischner recommendations are based on one study (15) with 234 PFNs and another study (16) with 794 typical and 125 atypical PFNs, with unspecified juxtapleural nodules, and they recommended no follow-up for PFNs or juxtapleural nodules that have triangular, oval, or lentiform shapes and smooth, sharp margins—even if the average dimension exceeds 6 mm or the nodule demonstrates interval growth. In the context of a lung cancer screening program, our recommendations are to have a 1-year follow-up with annual screening for CP-NCNs less than 10.0 mm with LOS or triangular shapes and smooth margins. These recommendations

Table 4: Results of Multivariable Logistic Regression Analysis for Size and Features of CP-NCNs Associated with Benignity

Parameter	Estimate	Standard Error	*P* Value	Odds Ratio
Size (mm)	−0.05	0.05	.24	0.95
Shape				
Triangular	6.45	2.36	.006	633.72
Lentiform, oval, or semicircular	3.94	0.94	<.001	51.46
Polygonal	3.19	0.94	<.001	24.37
Round	1.14	0.80	.15	3.13
Irregular	REF	REF	REF	REF
Margin				
Smooth	3.53	0.68	<.001	34.03
Nonsmooth	REF	REF	REF	REF
Nodule-pleural attachment				
Broad	0.13	0.35	.70	1.14
Narrow	REF	REF	REF	REF
Interaction terms				
Size × margin: smooth margin	−0.22	0.07	.001	0.80
Size × shape				
Triangular	−0.14	0.22	.52	0.87
Lentiform, oval, or semicircular	−0.09	0.08	.26	0.92
Polygonal	−0.31	0.11	.005	0.73
Round	0.04	0.07	.52	1.04

Note.—CP-NCN = noncalcified nodules attached to the costal pleura, REF = reference group for calculation of odds ratio.

are also consistent with the International Early Lung Cancer Action Program recommendation for participants enrolled in an annual screening program (26).

Our study had several limitations. Our number of malignancies of nine is small, so the use of traditional multivariable analysis can cause problems with model overfitting. To gain additional insight and to assess the independent contribution of each of the nodule features to the risk of lung cancer, we applied synthetic minority oversampling technique, which generated new synthetic samples from the existing lung cancer cases according to the nearest neighbor of these cases while undersampling non–lung cancer cases. It resulted in a more balanced data set with an increased number of lung cancer cases that were similar to the lung cancer cases in the original sample. Because this method created synthetic cases without considering the majority class (non–lung cancer cases), it may not alleviate the problem with overfitting in highly imbalanced data sets and could potentially result in a greater chance of class mixture. Therefore, we took a conservative approach and only based our follow-up recommendation for annual screening on all baseline CP-NCNs less than 10.0 mm in average diameter with LOS or triangular shapes and smooth margins, as all of these cases were benign in our study. Another limitation was that we limited our assessment to those CP-NCNs that had contact with the costal pleura. This is different from other definitions of PFNs that include nodules as far as 1 cm from the pleura (31). We also excluded nodules attached to the mediastinal and diaphragmatic pleurae, which were infrequent. Although these nodules might be assumed to behave like CP-NCNs, we believe a separate study with only such nodules would be better to address this issue. We did not assess the intra- and interobserver variability. However, our observations are in line with those performed by other radiologists interpreting low-dose CT screenings in the two largest randomized screening trials. Our database included participants with lower lung cancer risk, including never smokers. However, the results are the same when considering only the high-risk participants. In the future, artificial intelligence algorithms may reduce subjectivity in nodule characterization as well as minimize measurement variability.

In summary, we found that noncalcified nodules attached to the costal pleura smaller than 10.0 mm with lentiform, oval, or semicircular or triangular shapes and smooth margins identified at low-dose CT in the baseline round of screening were benign, regardless of the type of pleural attachment. Follow-up with annual screening, rather than more immediate work-up, is recommended.

Author contributions: Guarantor of integrity of entire study, C.I.H.; study concepts/study design or data acquisition or data analysis/interpretation, all authors; manuscript drafting or manuscript revision for important intellectual content, all authors; approval of final version of submitted manuscript, all authors; agrees to ensure any questions related to the work are appropriately resolved, all authors; literature research, Y.Z., R.Y., C.I.H., D.F.Y.; clinical studies, Y.Z., C.I.H., D.F.Y.; statistical analysis, Y.Z., R.Y., N.Y., C.I.H.; and manuscript editing, Y.Z., R.Y., N.Y., C.I.H., D.F.Y.

Disclosures of Conflicts of Interest: Y.Z. disclosed no relevant relationships. **R.Y.** disclosed no relevant relationships. **N.Y.** disclosed no relevant relationships. **C.I.H.** Activities related to the present article: disclosed no relevant relationships. Activities not related to the present article: disclosed no relevant relationships. Other relationships: disclosed patents and patent applications related to the evaluation of pulmonary nodules on chest CT scans, which are owned by Cornell Research Foundation, but has renounced any financial benefit from these patents, including royalties and any other proceeds related to the patents or patent applications owned by Cornell Research Foundation; author is president and serves on the board of the Early Diagnosis and Treatment Research but receives no compensation. **D.F.Y.** Activities related to the present article: disclosed no relevant relationships. Activities not related to the present article: receives payment as a GRAIL advisory board member; has patents planned, pending, or issued with General Electric; holds stock/stock options in Accumetra. Other relationships: disclosed no relevant relationships.

References

1. Kundel HL. Predictive value and threshold detectability of lung tumors. Radiology 1981;139(1):25–29.
2. Gurney JW, Lyddon DM, McKay JA. Determining the likelihood of malignancy in solitary pulmonary nodules with Bayesian analysis. Part II. Application. Radiology 1993;186(2):415–422.
3. Muhm JR, Miller WE, Fontana RS, Sanderson DR, Uhlenhopp MA. Lung cancer detected during a screening program using four-month chest radiographs. Radiology 1983;148(3):609–615.
4. Siegelman SS, Khouri NF, Leo FP, Fishman EK, Braverman RM, Zerhouni EA. Solitary pulmonary nodules: CT assessment. Radiology 1986;160(2):307–312.
5. Zerhouni EA, Stitik FP, Siegelman SS, et al. CT of the pulmonary nodule: a cooperative study. Radiology 1986;160(2):319–327.
6. Austin JH, Müller NL, Friedman PJ, et al. Glossary of terms for CT of the lungs: recommendations of the Nomenclature Committee of the Fleischner Society. Radiology 1996;200(2):327–331.
7. Henschke CI, McCauley DI, Yankelevitz DF, et al. Early Lung Cancer Action Project: overall design and findings from baseline screening. Lancet 1999;354(9173):99–105.
8. Henschke CI, Yankelevitz DF, Mirtcheva R, et al. CT screening for lung cancer: frequency and significance of part-solid and nonsolid nodules. AJR Am J Roentgenol 2002;178(5):1053–1057.
9. Henschke CI, Yankelevitz DF, Naidich DP, et al. CT screening for lung cancer: suspiciousness of nodules according to size on baseline scans. Radiology 2004;231(1):164–168.
10. Henschke CI, Yip R, Yankelevitz DF, Smith JP; International Early Lung Cancer Action Program Investigators*. Definition of a positive test result in computed tomography screening for lung cancer: a cohort study. Ann Intern Med 2013;158(4):246–252.
11. Sone S, Takashima S, Li F, et al. Mass screening for lung cancer with mobile spiral computed tomography scanner. Lancet 1998;351(9111):1242–1245.
12. Takashima S, Sone S, Li F, Maruyama Y, Hasegawa M, Kadoya M. Indeterminate solitary pulmonary nodules revealed at population-based CT screening of the lung: using first follow-up diagnostic CT to differentiate benign and malignant lesions. AJR Am J Roentgenol 2003;180(5):1255–1263.
13. Li F, Sone S, Abe H, Macmahon H, Doi K. Malignant versus benign nodules at CT screening for lung cancer: comparison of thin-section CT findings. Radiology 2004;233(3):793–798.
14. Xu DM, van der Zaag-Loonen HJ, Oudkerk M, et al. Smooth or attached solid indeterminate nodules detected at baseline CT screening in the NELSON study: cancer risk during 1 year of follow-up. Radiology 2009;250(1):264–272.
15. Ahn MI, Gleeson TG, Chan IH, et al. Perifissural nodules seen at CT screening for lung cancer. Radiology 2010;254(3):949–956.
16. de Hoop B, van Ginneken B, Gietema H, Prokop M. Pulmonary perifissural nodules on CT scans: rapid growth is not a predictor of malignancy. Radiology 2012;265(2):611–616.
17. Mets OM, Chung K, Scholten ET, et al. Incidental perifissural nodules on routine chest computed tomography: lung cancer or not? Eur Radiol 2018;28(3):1095–1101.
18. Han D, Heuvelmans MA, van der Aalst CM, et al. New Fissure-Attached Nodules in Lung Cancer Screening: A Brief Report From The NELSON Study. J Thorac Oncol 2020;15(1):125–129.
19. Callister ME, Baldwin DR, Akram AR, et al. British Thoracic Society guidelines for the investigation and management of pulmonary nodules. Thorax 2015;70(Suppl 2):ii1–ii54 [Published correction appears in Thorax 2015;70(12):1188.].
20. MacMahon H, Naidich DP, Goo JM, et al. Guidelines for Management of Incidental Pulmonary Nodules Detected on CT Images: From the Fleischner Society 2017. Radiology 2017;284(1):228–243.
21. Bueno J, Landeras L, Chung JH. Updated Fleischner Society Guidelines for Managing Incidental Pulmonary Nodules: Common Questions and Challenging Scenarios. RadioGraphics 2018;38(5):1337–1350.
22. American College of Radiology. Lung CT Screening Reporting & Data System (Lung-RADS) version 1.1. ACR web site. https://www.acr.org/Clinical-Resources/Reporting-and-Data-Systems/Lung-Rads. Published May 2019. Accessed May 22, 2020.
23. Hu M, Yip R, Yankelevitz DY, Henschke CI. CT screening for lung cancer: Frequency of enlarged adrenal glands identified in baseline and annual repeat rounds. Eur Radiol 2016;26(12):4475–4481.
24. Chen X, Li K, Yip R, et al. Hepatic steatosis in participants in a program of low-dose CT screening for lung cancer. Eur J Radiol 2017;94:174–179.
25. Zhu Y, Wang Y, Gioia WE, et al. Visual scoring of aortic valve calcifications on low-dose CT in lung cancer screening. Eur Radiol 2020;30(5):2658–2668.
26. I-ELCAP Investigators. International Early Lung Cancer Action Program: screening protocol. I-ELCAP website. https://www.ielcap.org/sites/default/files/I-ELCAP-protocol.pdf. Published July 6, 2016. Accessed May 22, 2020.
27. Kim HJ, Cho JY, Lee YJ, et al. Clinical Significance of Pleural Attachment and Indentation of Subsolid Nodule Lung Cancer. Cancer Res Treat 2019;51(4):1540–1548.
28. Takashima S, Maruyama Y, Hasegawa M, et al. CT findings and progression of small peripheral lung neoplasms having a replacement growth pattern. AJR Am J Roentgenol 2003;180(3):817–826.
29. Takashima S, Sone S, Li F, et al. Small solitary pulmonary nodules (< or =1 cm) detected at population-based CT screening for lung cancer: Reliable high-resolution CT features of benign lesions. AJR Am J Roentgenol 2003;180(4):955–964.
30. Yamamoto T, Kadoya N, Shirata Y, et al. Impact of tumor attachment to the pleura measured by a pretreatment CT image on outcome of stage I NSCLC treated with stereotactic body radiotherapy. Radiat Oncol 2015;10(1):35.
31. Schreuder A, van Ginneken B, Scholten ET, et al. Classification of CT Pulmonary Opacities as Perifissural Nodules: Reader Variability. Radiology 2018;288(3):867–875.
32. Detterbeck FC, Boffa DJ, Kim AW, et al. The Eighth Edition Lung Cancer Stage Classification. Chest 2017;151(1):193–203.